JOURNAL OF COMPUTATIONAL PHYSICS 97, 144–171 (1991)

The Electric Potential of a Macromolecule in a Solvent: A Fundamental Approach

ANDRÉ H. JUFFER,* EUGEN F. F. BOTTA,† BERT A. M. VAN KEULEN,†
AUKE VAN DER PLOEG,† AND HERMAN J. C. BERENDSEN*

*Laboratory of Physical Chemistry and †Department of Mathematics, University of Groningen, Groningen, The Netherlands

Received February 16, 1990; revised October 25, 1990

A general numerical method is presented to compute the electric potential for a macromolecule of arbitrary shape in a solvent with nonzero ionic strength. The model is based on a continuum description of the dielectric and screening properties of the system, which consists of a bounded internal region with discrete charges and an infinite external region. The potential obeys the Poisson equation in the internal region and the linearized Poisson–Boltzmann equation in the external region, coupled through appropriate boundary conditions. It is shown how this three-dimensional problem can be presented as a pair of coupled integral equations for the potential and the normal component of the electric field at the dielectric interface. These equations can be solved by a straightforward application of boundary element techniques. The solution involves the decomposition of a matrix that depends only on the geometry of the surface and not on the positions of the charges. With this approach the number of unknowns is reduced by an order of magnitude with respect to the usual finite difference methods. Special attention is given to the numerical inaccuracies resulting from charges which are located close to the interface; an adapted formulation is given for that case. The method is tested both for a spherical geometry, for which an exact solution is available, and for a realistic problem, for which a finite difference solution and experimental verification is available. The latter concerns the shift in acid strength (pK-values) of histidines in the copper-containing protein azurin on oxidation of the copper, for various values of the ionic strength. A general method is given to triangulate a macromolecular surface. The possibility is discussed to use the method presented here for a correct treatment of long-range electrostatic interactions in simulations of solvated macromolecules, which form an essential part of correct potentials of mean force.

1. INTRODUCTION

Electrostatic interactions play a very important role in the structural and functional properties of macromolecules, particularly in charged macromolecules as DNA and other polyelectrolytes. In proteins the correlated dipoles of alpha-helices produce long-range electrostatic effects with functional significance [1–3]. The presence of a solvent with high dielectric constant, such as water, modifies the interactions between charges considerably beyond the direct Coulomb term, as a result of the *reaction field* due to the medium. The influence of the reaction field on the energy of a charge is the major term determining solubility properties, as was

0021-9991/91 $3.00

already realized by Born [4]. If the medium is an electrolyte solution, additional screening occurs due to the charge density in the medium resulting from the Boltzmann distribution of ions in the electric potential. Only simple geometries were used in early attempts to apply the screened reaction field to solvated molecules [5] and proteins [6].

For molecular dynamics or Monte Carlo simulations of solvated macromolecules the proper treatment of electrostatic interactions is critical. The only reliable method available today is the incorporation of a sufficient number of explicit solvent molecules at the expense of an additional order of magnitude in computer time. As an approximation, Warshel [7] has used shells of polarisable *Langevin dipoles* to replace the solvent. *Ad hoc* solutions as distance-dependent dielectric constants and modified charges to mimic the reaction field effects are commonly used, but are not sufficiently accurate.

Continuum Equations

An alternative approach, on which we now concentrate, is a continuum description of the dielectric properties of the system. If accurate numerical solutions are obtained, the long-range electrostatic behaviour will be described correctly and only short-range corrections will be necessary to account for the atomic detail. We shall assume that the region inside the macromolecule has a uniform dielectric constant ε_1 and that all explicit charges are located within this region. The outside region has a uniform dielectric constant ε_2 and represents an ideal ionic solution with a given ionic strength and behaving according to the linearized Poisson–Boltzmann equation. The dielectric response is assumed to be linear in both regions. These assumptions are valid when the electric fields are small and may break down in the neighbourhood of a strongly polarizing charge, or in the case that specific structural ordering of the solvent molecules occurs. In such cases, however, the solvent molecules should be explicitly treated in the model and not generalized into the continuum.

Formulation of the Problem

The continuum description can be formulated as follows. Consider a smooth closed two-dimensional surface Σ that contains the macromolecule and roughly follows its shape. Inside the surface (region I) there are N charges q_i at points $\mathbf{r}_i$, $i = 1, 2, ..., N$. Here the dielectric constant is ε_1 and the electric potential is φ, while outside the surface (region II) the dielectric constant is $\varepsilon_2 = \varepsilon\varepsilon_1$ and the potential is ψ. Consequently φ satisfies the Poisson equation

$$\nabla^2\varphi(\mathbf{r}) = -\sum_{i=1}^{N} q_i\,\delta(\mathbf{r}-\mathbf{r}_i)/\varepsilon_1, \qquad \mathbf{r} \in \text{region I},$$

where $\delta(\mathbf{r}-\mathbf{r}_i)$ is the delta distribution at $\mathbf{r}_i$. The outside potential ψ satisfies the linearized Poisson–Boltzmann equation

$$\nabla^2\psi(\mathbf{r}) = \kappa^2\psi(\mathbf{r}), \qquad \mathbf{r} \in \text{region II},$$

where κ is the inverse Debye screening length defined by

$$\kappa^2 = \frac{2IF^2}{\varepsilon_2 RT}, \qquad \text{with} \quad I = \frac{1}{2}\sum_i c_i z_i^2.$$

Here I is the ionic strength, F the Faraday (96485.309 C mole^{-1}), ε_2 the dielectric constant of the medium, equal to its relative dielectric constant (80 for water) multiplied by the permittivity of vacuum ($\varepsilon_0 = 8.854187817 \times 10^{-12}$ Fm^{-1}), R the gas constant (8.314510 J mole^{-1}K^{-1}), T the absolute temperature in K, c_i the concentration of the ith ionic species in moles per cubic meter, and z_i its charge in units of the elementary charge.
The potentials φ and ψ must satisfy the following boundary conditions:

(i) Continuity of the electric potential: $\varphi(\mathbf{r}) = \psi(\mathbf{r})$ on Σ,

(ii) Continuity of the normal component of the dielectric displacement: $(\partial\varphi/\partial n)(\mathbf{r}) = \varepsilon(\partial\psi/\partial n)(\mathbf{r})$ on Σ, where n is the outward unit normal to the surface at $\mathbf{r}$ and $\varepsilon = \varepsilon_2/\varepsilon_1$.

Finally, under the extra condition that ψ satisfies regularity conditions at infinity, i.e., $|\mathbf{r}|\,\psi(\mathbf{r})$ and $|\mathbf{r}|^2\,\nabla\psi(\mathbf{r})$ are bounded for $|\mathbf{r}|$ tending to infinity, the problem has a unique solution. Without loss of generality we may take $\varepsilon_1 = 1$, which implies a scaling of charges.

Finite-Difference Methods

Analytic solutions are only available in special cases (e.g., if the surface is a sphere [8]. Also the series expansion of the Poisson–Green's function, given by Shaw [9] seems in practice not applicable to general surfaces). Therefore several numerical methods have been developed (for a review see Davis and McCammon [10]). Warwicker and Watson [11] used a finite-difference method for the case $\kappa = 0$ to solve the resulting Poisson equation directly. Klapper *et al.* [12] and Gilson *et al.* [13] used a finite-difference method for the general case with κ non-zero. A drawback of finite-difference methods is that the local potential due to nearby charges cannot be accurately represented by the solution on the grid. Therefore Nakamura [14] has combined the direct Coulomb potential with a reaction potential calculated by a finite-difference method on a grid. In all these methods a three-dimensional grid is imposed to partition the molecular interior and a sufficiently large portion of the surrounding solvent into small volume elements. This typically leads to a large number of unknown parameters, which imposes high demands on computer power and storage.

Boundary Element Methods

Boundary element methods exploit the fact that in many problems the differential equations can be transformed into a set of boundary integral equations. This reduces the dimension of the problem by one and eliminates the difficulties associated with domains extending to infinity. For the general treatment of bound-

ary element methods we refer to standard text books [15, 16]. Zauhar and Morgan [17, 18] have formulated the problem for $\kappa = 0$ as an integral equation on the surface with one unknown function, representing a polarization charge density. The potentials inside and outside the surface can be expressed in this unknown function, so once this function has been calculated the problem is solved and the regularity conditions at infinity are treated correctly. This boundary element approach allows for better surface approximations than the finite-difference method. Furthermore, the number of unknowns is reduced by an order of magnitude since this method involves the use of two-dimensional surface elements instead of three-dimensional volume elements. Moreover, there is no difficulty in representing the charges because, as will be shown later on, they only appear on the right side of a matrix equation $\mathbf{Ax} = \mathbf{b}$, where $\mathbf{x}$ contains the unknown parameters of the induced surface charge. This yields another advantage over the finite-difference method in case many charge distributions are considered for a given shape, as in molecular dynamics simulations: as long as the shape of Σ does not change, different positions or magnitudes of the charges only have an effect on $\mathbf{b}$, whereas in the finite-difference method a new system of equations must be solved for every new charge distribution. The method of Zauhar and Morgan has been applied to the protein papain by Dijkman [19].

Unfortunately, Zauhar and Morgan could only obtain the integral formulation in the case of $\kappa = 0$, i.e., when the solvent obeys the Laplace equation rather than the linearized Poisson–Boltzmann equation. In 1987 Zauhar stated that "if counter ion charge is to be included in the induced polarization charge model, it will be necessary to introduce some sort of three-dimensional element" [20]. This was in fact done by Rashin [21], who included a counter ion distribution in a boundary element description by extending the finite elements to three-dimensional space. The restriction to $\kappa = 0$ would deny the advantages of the boundary element method to many applications of practical interest where the ionic strength has an important influence on the electric potential.

However, in 1983 van der Eerden [22] considered the general case including ionic strength and proposed a formulation based on a Green's function formalism that yielded a pair of integral equations over the surface. In addition to the surface charge distribution (which is equivalent to the distribution of the normal component of the electric field), a second unknown appears which is the potential at the surface. This solves the problem in principle, but the method was not further worked out at the time and the equations of van der Eerden still contained an undetermined limit due to a singularity, which prevented the successful application of any numerical procedure.

The General Boundary Element Method

We have been able to reformulate the integral equations in such a way that no singularity appears. This derivation, given in Section 2, yields two integral equations, (2.17) and (2.18), which can be solved for the two unknowns $\varphi(\mathbf{r})$ and $h(\mathbf{r}) = (\partial\varphi/\partial n)(\mathbf{r})$, $\mathbf{r} \in \Sigma$. The internal and external potential can then be obtained from

$\varphi(\mathbf{r})$, $h(\mathbf{r})$, and a source term. For the case $\kappa = 0$ only one of the equations is needed. In Section 3 the integral equations are numerically solved by transformation into a set of linear equations. It is shown in Appendix A how the difficulties can be resolved that arise when a charge approaches Σ too closely. Section 4 compares numerical results with the exact solution for one charge placed eccentrically in a sphere. Section 5 describes the application to the copper-containing protein *azurin*, for which pK-shifts of histidine groups on oxidation of the copper are known experimentally, and for which a finite-element solution has been published. In Section 6 the applicability of the method is discussed. In Section 7 we conclude with a comprehensive summary of the relevant equations.

2. Formulation of the Integral Equations

With well-known methods from mathematical physics (e.g., [23]) the problem can be transformed into two coupled linear integral equations as was announced in the Introduction. First, by using the fundamental solutions to the Poisson and the linearized Poisson–Boltzmann equation, the potentials φ and ψ can be expressed in terms of the functions $\varphi(\mathbf{r})$ and $(\partial\varphi/\partial n)(\mathbf{r})$ and the functions $\psi(\mathbf{r})$ and $(\partial\psi/\partial n)(\mathbf{r})$ respectively, where $\mathbf{r}$ is on Σ and $\mathbf{n}$ is again the outward unit normal to Σ at $\mathbf{r}$.

From now on $\mathbf{r}_0^-$ will be a point inside Σ, $\mathbf{r}_0^+$ a point outside Σ, and $\mathbf{r}_0$ will be on Σ. The fundamental solution to the Poisson equation with singularity in $\mathbf{s}$ satisfies

$$\nabla^2 F(\mathbf{r};\mathbf{s}) = -\delta(\mathbf{r}-\mathbf{s}) \tag{2.1}$$

and is given by

$$F(\mathbf{r};\mathbf{s}) = 1/(4\pi\,|\mathbf{r}-\mathbf{s}|).$$

In the region inside Σ we have the following equation for φ:

$$\nabla^2\varphi(\mathbf{r}) = -\sum_{i=1}^{N} q_i\,\delta(\mathbf{r}-\mathbf{r}_i). \tag{2.2}$$

By taking for $\mathbf{s}$ a point $\mathbf{r}_0^-$ inside Σ, multiplying $\varphi(\mathbf{r})$ with (2.1), subtracting $F(\mathbf{r};\mathbf{r}_0^-)$ times (2.2), and applying Green's second theorem on the volume inside Σ minus small balls with radius ρ around $\mathbf{r}_0^-$ and $\mathbf{r}_i$ and with ρ tending to zero, we obtain an expression for $\varphi(\mathbf{r}_0^-)$ in $\varphi(\mathbf{r})$ and $(\partial\varphi/\partial n)(\mathbf{r})$ on Σ,

$$\varphi(\mathbf{r}_0^-) = \int\!\!\int_{\Sigma}\left[F(\mathbf{r};\mathbf{r}_0^-)\frac{\partial\varphi}{\partial n}(\mathbf{r}) - \varphi(\mathbf{r})\frac{\partial F}{\partial n}(\mathbf{r};\mathbf{r}_0^-)\right]d\mathbf{r} + \sum_{i=1}^{N} q_i F(\mathbf{r}_i;\mathbf{r}_0^-). \tag{2.3}$$

Here $F(\mathbf{r};\mathbf{r}_0^-)$ is in fact the potential in $\mathbf{r}_0^-$ of a charge in $\mathbf{r}$, whereas $(\partial F/\partial n)(\mathbf{r};\mathbf{r}_0^-)$ is the potential in $\mathbf{r}_0^-$ of a dipole in $\mathbf{r}$ with direction $\mathbf{n}$, since

$$\frac{\partial F}{\partial n}(\mathbf{r};\mathbf{s}) = -(\mathbf{n}\cdot(\mathbf{r}-\mathbf{s}))/(4\pi\,|\mathbf{r}-\mathbf{s}|^3).$$

So $\varphi(\mathbf{r}_0^-)$ is the sum of the potentials of a source term, a simple layer, and a double layer at the surface. Similarly, ψ can be expressed in terms of the functions $\psi(\mathbf{r})$ and $(\partial\psi/\partial n)(\mathbf{r})$ on Σ, using the fundamental solution to the linearized Poisson–Boltzmann equation with singularity in $\mathbf{s}$,

$$P(\mathbf{r};\mathbf{s}) = e^{-\kappa|\mathbf{r}-\mathbf{s}|}F(\mathbf{r};\mathbf{s}), \tag{2.4}$$

satisfying

$$\nabla^2 P(\mathbf{r};\mathbf{s}) = \kappa^2 P(\mathbf{r};\mathbf{s}) - \delta(\mathbf{r}-\mathbf{s}). \tag{2.5}$$

So with $\mathbf{s} = \mathbf{r}_0^+$ and

$$\nabla^2\psi(\mathbf{r}) = \kappa^2\psi(\mathbf{r}), \tag{2.6}$$

applying Green's second theorem on the region outside Σ now gives

$$\psi(\mathbf{r}_0^+) = \iint_\Sigma \left[-P(\mathbf{r};\mathbf{r}_0^+)\frac{\partial\psi}{\partial n}(\mathbf{r}) + \psi(\mathbf{r})\frac{\partial P}{\partial n}(\mathbf{r};\mathbf{r}_0^+)\right] d\mathbf{r}. \tag{2.7}$$

Note that here the regularity condition for ψ is used and that (2.7) is the sum of the modified potential of a simple layer, see (2.4), and the modified potential of a double layer at the surface:

$$\frac{\partial P}{\partial n}(\mathbf{r};\mathbf{s}) = (1+\kappa|\mathbf{r}-\mathbf{s}|)\,e^{-\kappa|\mathbf{r}-\mathbf{s}|}\frac{\partial F}{\partial n}(\mathbf{r};\mathbf{s}).$$

Now in (2.3) and (2.7) the limits for $\mathbf{r}_0^\pm$ to Σ can be taken using the properties of simple and double layers ([23]). So

$$\lim_{\mathbf{r}_0^- \uparrow \mathbf{r}_0} \varphi(\mathbf{r}_0^-) = \iint_\Sigma \left[F(\mathbf{r};\mathbf{r}_0)\frac{\partial\varphi}{\partial n}(\mathbf{r}) - \varphi(\mathbf{r})\frac{\partial F}{\partial n}(\mathbf{r};\mathbf{r}_0)\right] d\mathbf{r} + \frac{1}{2}\varphi(\mathbf{r}_0) + \sum_{i=1}^{N} q_i F(\mathbf{r}_i;\mathbf{r}_0), \tag{2.8}$$

where $\mathbf{r}_0$ is on Σ as stated above and

$$\lim_{\mathbf{r}_0^+ \downarrow \mathbf{r}_0} \psi(\mathbf{r}_0^+) = \iint_\Sigma \left[-P(\mathbf{r};\mathbf{r}_0)\frac{\partial\psi}{\partial n}(\mathbf{r}) + \psi(\mathbf{r})\frac{\partial P}{\partial n}(\mathbf{r};\mathbf{r}_0)\right] d\mathbf{r} + \frac{1}{2}\psi(\mathbf{r}_0). \tag{2.9}$$

Note that although $F(\mathbf{r};\mathbf{r}_0)$ and $(\partial F/\partial n)(\mathbf{r};\mathbf{r}_0)$ are weakly singular in $\mathbf{r}_0$, they are still integrable over Σ and the same holds for $P(\mathbf{r};\mathbf{r}_0)$ and $(\partial P/\partial n)(\mathbf{r};\mathbf{r}_0)$. Using the boundary conditions

$$\lim_{\mathbf{r}_0^- \uparrow \mathbf{r}_0} \varphi(\mathbf{r}_0^-) = \varphi(\mathbf{r}_0) = \psi(\mathbf{r}_0) = \lim_{\mathbf{r}_0^+ \downarrow \mathbf{r}_0} \psi(\mathbf{r}_0^+) \tag{2.10}$$

and

$$\frac{\partial \varphi}{\partial n}(\mathbf{r}_0) = \varepsilon \frac{\partial \psi}{\partial n}(\mathbf{r}_0) \tag{2.11}$$

and adding (2.8) and ε times (2.9), the first integral equation is obtained:

$$\frac{1}{2}(1+\varepsilon)\,\varphi(\mathbf{r}_0) = \iint_{\Sigma} \{F(\mathbf{r};\mathbf{r}_0) - P(\mathbf{r};\mathbf{r}_0)\} \frac{\partial \varphi}{\partial n}(\mathbf{r})\, d\mathbf{r} + \iint_{\Sigma} \left\{ \varepsilon \frac{\partial P}{\partial n}(\mathbf{r};\mathbf{r}_0) - \frac{\partial F}{\partial n}(\mathbf{r};\mathbf{r}_0) \right\} \varphi(\mathbf{r})\, d\mathbf{r} + \sum_i q_i F(\mathbf{r}_i;\mathbf{r}_0) \tag{2.12}$$

with $\varphi(\mathbf{r})$ and $(\partial\varphi/\partial n)(\mathbf{r})$ the unknown functions on Σ.

In order to derive a second integral equation for these functions, we have to consider the normal derivatives in (2.3) and (2.7). Let $\mathbf{n}_0$ be the outward unit normal at the point $\mathbf{r}_0$ on Σ. In (2.3) and (2.7) we take the derivative of $\varphi(\mathbf{r}_0^-)$ and $\psi(\mathbf{r}_0^+)$ in the direction $\mathbf{n}_0$. So with

$$\frac{\partial}{\partial n_0} = \mathbf{n}_0 \cdot \nabla_{\mathbf{r}_0^{\pm}},$$

we find

$$\frac{\partial \varphi}{\partial n_0}(\mathbf{r}_0^-) = \iint_{\Sigma} \left[\frac{\partial F}{\partial n_0}(\mathbf{r};\mathbf{r}_0^-) \frac{\partial \varphi}{\partial n}(\mathbf{r}) - \varphi(\mathbf{r}) \frac{\partial^2 F}{\partial n_0\, \partial n}(\mathbf{r};\mathbf{r}_0^-) \right] d\mathbf{r} + \sum_{i=1}^{N} q_i \frac{\partial F}{\partial n_0}(\mathbf{r}_i;\mathbf{r}_0^-) \tag{2.13}$$

and

$$\frac{\partial \psi}{\partial n_0}(\mathbf{r}_0^+) = \iint_{\Sigma} \left[-\frac{\partial P}{\partial n_0}(\mathbf{r};\mathbf{r}_0^+) \frac{\partial \psi}{\partial n}(\mathbf{r}) + \psi(\mathbf{r}) \frac{\partial^2 P}{\partial n_0\, \partial n}(\mathbf{r};\mathbf{r}_0^+) \right] d\mathbf{r}. \tag{2.14}$$

Here

$$\frac{\partial F}{\partial n_0}(\mathbf{r};\mathbf{s}) = \cos\theta_0/(4\pi\,|\mathbf{r}-\mathbf{s}|^2)$$

$$\frac{\partial P}{\partial n_0}(\mathbf{r};\mathbf{s}) = (1+\kappa\,|\mathbf{r}-\mathbf{s}|)\, e^{-\kappa|\mathbf{r}-\mathbf{s}|} \frac{\partial F}{\partial n_0}(\mathbf{r};\mathbf{s})$$

$$\frac{\partial^2 F}{\partial n_0\, \partial n}(\mathbf{r};\mathbf{s}) = ((\mathbf{n}_0 \cdot \mathbf{n}) - 3\cos\theta\cos\theta_0)/(4\pi\,|\mathbf{r}-\mathbf{s}|^3)$$

$$\frac{\partial^2 P}{\partial n_0\, \partial n}(\mathbf{r};\mathbf{s}) = (1+\kappa\,|\mathbf{r}-\mathbf{s}|)\, e^{-\kappa|\mathbf{r}-\mathbf{s}|} \frac{\partial^2 F}{\partial n_0\, \partial n}(\mathbf{r};\mathbf{s}) - \kappa^2 e^{-\kappa|\mathbf{r}-\mathbf{s}|} \cos\theta\cos\theta_0/(4\pi\,|\mathbf{r}-\mathbf{s}|)$$

with

$$\cos\theta = (\mathbf{n}\cdot(\mathbf{r}-\mathbf{s}))/|\mathbf{r}-\mathbf{s}|$$

and

$$\cos\theta_0 = (\mathbf{n}_0\cdot(\mathbf{r}-\mathbf{s}))/|\mathbf{r}-\mathbf{s}|.$$

Taking the limits for $\mathbf{r}_0^{\pm}\to\Sigma$, i.e., for $\mathbf{r}_0^{\pm}\to\mathbf{r}_0$, is now far more complicated then in the derivation of the first integral equation. This is caused by the behaviour of $(\partial^2 F/\partial n_0\,\partial n)(\mathbf{r};\mathbf{r}_0^-)$ and $\partial^2 P/\partial n_0\,\partial n(\mathbf{r};\mathbf{r}_0^+)$, where the first is the normal component of the field of a dipole. These functions are not integrable over Σ when $\mathbf{r}_0^{\pm}$ is on Σ but it turns out that the difference is.

Obviously $(\partial F/\partial n_0)(\mathbf{r};\mathbf{s})$ is again the potential of a dipole. It is known (e.g., [23]) that the normal derivative of the potential of a double layer is continuous across the layer, so

$$\lim_{\mathbf{r}_0^-\uparrow\mathbf{r}_0}\frac{\partial}{\partial n_0}\iint_{\Sigma}\varphi(\mathbf{r})\frac{\partial F}{\partial n}(\mathbf{r};\mathbf{r}_0^-)\,d\mathbf{r} = \lim_{\mathbf{r}_0^+\downarrow\mathbf{r}_0}\frac{\partial}{\partial n_0}\iint_{\Sigma}\varphi(\mathbf{r})\frac{\partial F}{\partial n}(\mathbf{r};\mathbf{r}_0^+)\,d\mathbf{r}.$$

Let

$$g(\mathbf{r};\mathbf{s}) = \frac{\partial^2 P}{\partial n_0\,\partial n}(\mathbf{r};\mathbf{s}) - \frac{\partial^2 F}{\partial n_0\,\partial n}(\mathbf{r};\mathbf{s});$$

then for $|\mathbf{r}-\mathbf{s}|\to 0$,

$$g(\mathbf{r};\mathbf{s}) = \kappa^2(\cos\theta\cos\theta_0 - (\mathbf{n}_0\cdot\mathbf{n}))/(8\pi\,|\mathbf{r}-\mathbf{s}|) + \kappa^3(\mathbf{n}_0\cdot\mathbf{n})/12\pi + O(|\mathbf{r}-\mathbf{s}|),$$

so $g(\mathbf{r};\mathbf{r}_0)$ as a function of $\mathbf{r}$ is integrable over Σ,

$$\lim_{\mathbf{r}_0^{\pm}\to\mathbf{r}_0}\iint_{\Sigma} g(\mathbf{r};\mathbf{r}_0^{\pm})\,d\mathbf{r} = \iint_{\Sigma} g(\mathbf{r};\mathbf{r}_0)\,d\mathbf{r}$$

and

$$\begin{aligned}
&\lim_{\mathbf{r}_0^+\downarrow\mathbf{r}_0}\frac{\partial}{\partial n_0}\iint_{\Sigma}\varphi(\mathbf{r})\frac{\partial P}{\partial n}(\mathbf{r};\mathbf{r}_0^+)\,d\mathbf{r} - \lim_{\mathbf{r}_0^-\uparrow\mathbf{r}_0}\frac{\partial}{\partial n_0}\iint_{\Sigma}\varphi(\mathbf{r})\frac{\partial F}{\partial n}(\mathbf{r};\mathbf{r}_0^-)\,d\mathbf{r}\\
&\quad= \lim_{\mathbf{r}_0^+\downarrow\mathbf{r}_0}\frac{\partial}{\partial n_0}\iint_{\Sigma}\varphi(\mathbf{r})\frac{\partial P}{\partial n}(\mathbf{r};\mathbf{r}_0^+)\,d\mathbf{r} - \lim_{\mathbf{r}_0^+\downarrow\mathbf{r}_0}\frac{\partial}{\partial n_0}\iint_{\Sigma}\varphi(\mathbf{r})\frac{\partial F}{\partial n}(\mathbf{r};\mathbf{r}_0^+)\,d\mathbf{r}\\
&\quad= \lim_{\mathbf{r}_0^+\downarrow\mathbf{r}_0}\frac{\partial}{\partial n_0}\iint_{\Sigma}\varphi(\mathbf{r})\left\{\frac{\partial P}{\partial n}(\mathbf{r};\mathbf{r}_0^+) - \frac{\partial F}{\partial n}(\mathbf{r};\mathbf{r}_0^+)\right\}d\mathbf{r}\\
&\quad= \iint_{\Sigma}\varphi(\mathbf{r})\,g(\mathbf{r};\mathbf{r}_0)\,d\mathbf{r}. \qquad (2.15)
\end{aligned}$$

Taking the limits for $\mathbf{r}_0^{\pm} \to \mathbf{r}_0$ in (2.13) and (2.14) the first term in the integrand can be treated as before; hence

$$\lim_{\mathbf{r}_0^- \uparrow \mathbf{r}_0} \frac{\partial \varphi}{\partial n_0}(\mathbf{r}_0^-) = \iint_{\Sigma} \frac{\partial F}{\partial n_0}(\mathbf{r};\mathbf{r}_0)\frac{\partial \varphi}{\partial n}(\mathbf{r})\,d\mathbf{r} + \frac{1}{2}\frac{\partial \varphi}{\partial n}(\mathbf{r}_0) + \sum_{i=1}^{N} q_i \frac{\partial F}{\partial n_0}(\mathbf{r}_i;\mathbf{r}_0)$$
$$- \lim_{\mathbf{r}_0^- \uparrow \mathbf{r}_0} \frac{\partial}{\partial n_0} \iint_{\Sigma} \varphi(\mathbf{r}) \frac{\partial F}{\partial n}(\mathbf{r};\mathbf{r}_0^-)\,d\mathbf{r}$$

and

$$\lim_{\mathbf{r}_0^+ \downarrow \mathbf{r}_0} \frac{\partial \psi}{\partial n_0}(\mathbf{r}_0^+) = \iint_{\Sigma} -\frac{\partial P}{\partial n_0}(\mathbf{r};\mathbf{r}_0)\frac{\partial \psi}{\partial n}(\mathbf{r})\,d\mathbf{r} + \frac{1}{2}\frac{\partial \psi}{\partial n}(\mathbf{r}_0)$$
$$+ \lim_{\mathbf{r}_0^+ \downarrow \mathbf{r}_0} \frac{\partial}{\partial n_0} \iint_{\Sigma} \varphi(\mathbf{r}) \frac{\partial P}{\partial n}(\mathbf{r};\mathbf{r}_0^+)\,d\mathbf{r}$$

After summation of these relations and using (2.15),

$$\lim_{\mathbf{r}_0^- \uparrow \mathbf{r}_0} \frac{\partial \varphi}{\partial n_0}(\mathbf{r}_0^-) = \frac{\partial \varphi}{\partial n_0}(\mathbf{r}_0) = \frac{\partial \varphi}{\partial n}(\mathbf{r}_0), \qquad \lim_{\mathbf{r}_0^+ \downarrow \mathbf{r}_0} \frac{\partial \psi}{\partial n_0}(\mathbf{r}_0^+) = \frac{\partial \psi}{\partial n_0}(\mathbf{r}_0) = \frac{\partial \psi}{\partial n}(\mathbf{r}_0),$$

together with the boundary conditions (2.10) and (2.11), we obtain the second integral equation

$$\frac{1}{2}(1 + 1/\varepsilon)\frac{\partial \varphi}{\partial n}(\mathbf{r}_0) = \iint_{\Sigma} \left[\left\{ \frac{\partial F}{\partial n_0}(\mathbf{r};\mathbf{r}_0) - \frac{\partial P}{\partial n_0}(\mathbf{r};\mathbf{r}_0)/\varepsilon \right\} \frac{\partial \varphi}{\partial n}(\mathbf{r}) + \varphi(\mathbf{r})\, g(\mathbf{r};\mathbf{r}_0) \right] d\mathbf{r}$$
$$+ \sum_{i=1}^{N} q_i \frac{\partial F}{\partial n_0}(\mathbf{r}_i;\mathbf{r}_0). \tag{2.16}$$

It is essential to use the right combination of the two limits, since otherwise the resulting integrands are not integrable over Σ.

In general a numerical method must be used to solve the integral equations (2.12) and (2.16) for the unknown functions $\varphi(\mathbf{r})$ and $(\partial\varphi/\partial n)(\mathbf{r})$. To stress the fact that both functions on Σ are independent, we will denote in the sequel of this paper $(\partial\varphi/\partial n)(\mathbf{r})$ by $h(\mathbf{r})$. With the notation

$$L_1(\mathbf{r};\mathbf{r}_0) = \varepsilon \frac{\partial P}{\partial n}(\mathbf{r};\mathbf{r}_0) - \frac{\partial F}{\partial n}(\mathbf{r};\mathbf{r}_0)$$
$$L_2(\mathbf{r};\mathbf{r}_0) = F(\mathbf{r};\mathbf{r}_0) - P(\mathbf{r};\mathbf{r}_0)$$
$$L_3(\mathbf{r};\mathbf{r}_0) = g(\mathbf{r};\mathbf{r}_0)$$
$$L_4(\mathbf{r};\mathbf{r}_0) = \frac{\partial F}{\partial n_0}(\mathbf{r};\mathbf{r}_0) - \frac{\partial P}{\partial n_0}(\mathbf{r};\mathbf{r}_0)/\varepsilon,$$

the integral equations (2.12) and (2.16) can be written as

$$\frac{1}{2}(1+\varepsilon)\,\varphi(\mathbf{r}_0)-\iint_{\Sigma}[L_1(\mathbf{r};\mathbf{r}_0)\,\varphi(\mathbf{r})+L_2(\mathbf{r};\mathbf{r}_0)\,h(\mathbf{r})]\,d\mathbf{r}=\sum_i q_i F(\mathbf{r}_i;\mathbf{r}_0) \quad (2.17)$$

and

$$\frac{1}{2}(1+1/\varepsilon)\,h(\mathbf{r}_0)-\iint_{\Sigma}[L_3(\mathbf{r};\mathbf{r}_0)\,\varphi(\mathbf{r})+L_4(\mathbf{r};\mathbf{r}_0)\,h(\mathbf{r}_0)]\,d\mathbf{r}=\sum_i q_i\frac{\partial F}{\partial n_0}(\mathbf{r}_i;\mathbf{r}_0). \quad (2.18)$$

This is the final pair of integral equations from which $\varphi(\mathbf{r}_0)$ and $h(\mathbf{r}_0)$ on Σ can be solved. Afterwards we can obtain the potentials inside and outside Σ using the formulas (2.3) and (2.7).

In the special case $\kappa=0$ we have $P(\mathbf{r};\mathbf{s})\equiv F(\mathbf{r};\mathbf{s})$; thus L_2 becomes zero and the integral equation (2.17) contains only φ as an unknown function. Therefore we wish to have formulas by which we can calculate for $\kappa=0$ the potentials using only φ on Σ.

Using the formulas (2.5) and (2.6), taking for $\mathbf{s}$ an interior point $\mathbf{r}_0^-$, and applying Green's second theorem on the area outside Σ yields

$$\iint_{\Sigma}\left[P(\mathbf{r};\mathbf{r}_0^-)\frac{\partial\psi}{\partial n}(\mathbf{r})-\frac{\partial P}{\partial n}(\mathbf{r};\mathbf{r}_0^-)\,\psi(\mathbf{r})\right]d\mathbf{r}=0.$$

By using the boundary conditions on Σ we can rewrite this last equation as

$$\iint_{\Sigma}\left[P(\mathbf{r};\mathbf{r}_0^-)\,h(\mathbf{r})/\varepsilon-\frac{\partial P}{\partial n}(\mathbf{r};\mathbf{r}_0^-)\,\varphi(\mathbf{r})\right]d\mathbf{r}=0. \quad (2.19)$$

Subtracting ε times (2.19) from (2.3) results in

$$\varphi(\mathbf{r}_0^-)=\iint_{\Sigma}[L_1(\mathbf{r};\mathbf{r}_0^-)\,\varphi(\mathbf{r})+L_2(\mathbf{r};\mathbf{r}_0^-)\,h(\mathbf{r})]\,d\mathbf{r}+\sum_i q_i F(\mathbf{r}_i;\mathbf{r}_0^-). \quad (2.20)$$

We also wish to derive a similar equation for the potential outside Σ. By taking for $\mathbf{s}$ an exterior point $\mathbf{r}_0^+$, multiplying $\varphi(\mathbf{r})$ with (2.1), subtracting $F(\mathbf{r};\mathbf{r}_0^+)$ times (2.2), and applying Green's second theorem on the volume inside Σ minus small balls with radius ρ around $\mathbf{r}_i$ and with ρ tending to zero, we obtain

$$\iint_{\Sigma}\left[\varphi(\mathbf{r})\frac{\partial F}{\partial n}(\mathbf{r};\mathbf{r}_0^+)-F(\mathbf{r};\mathbf{r}_0^+)\,h(\mathbf{r})\right]d\mathbf{r}=\sum_{i=1}^{N} q_i F(\mathbf{r}_i;\mathbf{r}_0^+). \quad (2.21)$$

By using the boundary conditions on Σ we can derive from (2.7)

$$\varepsilon\psi(\mathbf{r}_0^+)=\iint_{\Sigma}\left[\varepsilon\varphi(\mathbf{r})\frac{\partial P}{\partial n}(\mathbf{r};\mathbf{r}_0^+)-P(\mathbf{r};\mathbf{r}_0^+)\,h(\mathbf{r})\right]d\mathbf{r}. \quad (2.22)$$

Summation of (2.22) and (2.21) yields

$$\varepsilon\psi(\mathbf{r}_0^+) = \iint_\Sigma [L_1(\mathbf{r};\mathbf{r}_0^+)\,\varphi(\mathbf{r}) + L_2(\mathbf{r};\mathbf{r}_0^+)\,h(\mathbf{r})]\,d\mathbf{r} + \sum_i q_i F(\mathbf{r}_i;\mathbf{r}_0^+). \tag{2.23}$$

For $\kappa = 0$ Eqs. (2.17), (2.20), and (2.23) respectively reduce to

$$\frac{1}{2}(1+\varepsilon)\,\varphi(\mathbf{r}_0) = (\varepsilon-1)\iint_\Sigma \frac{\partial F}{\partial n}(\mathbf{r};\mathbf{r}_0)\,\varphi(\mathbf{r})\,d\mathbf{r} + \sum_i q_i F(\mathbf{r}_i;\mathbf{r}_0) \tag{2.24}$$

$$\varphi(\mathbf{r}_0^-) = (\varepsilon-1)\iint_\Sigma \frac{\partial F}{\partial n}(\mathbf{r};\mathbf{r}_0^-)\,\varphi(\mathbf{r})\,d\mathbf{r} + \sum_i q_i F(\mathbf{r}_i;\mathbf{r}_0^-) \tag{2.25}$$

and

$$\varepsilon\psi(\mathbf{r}_0^+) = (\varepsilon-1)\iint_\Sigma \frac{\partial F}{\partial n}(\mathbf{r};\mathbf{r}_0^+)\,\varphi(\mathbf{r})\,d\mathbf{r} + \sum_i q_i F(\mathbf{r}_i;\mathbf{r}_0^+). \tag{2.26}$$

So in case $\kappa = 0$ we can solve φ on Σ from the single integral equation (2.24). Afterwards, we can obtain the potentials inside and outside Σ from (2.25) and (2.26). It is also possible to derive equations which use only h on Σ when $\kappa = 0$. Zauhar and Morgan used a function on Σ which differs only a constant factor from h (see [17, 18]). In Section 4 we will see that on Σ the approximation of h is more complicated than that of φ. In the sequel of this paper we will use (2.20) and (2.23) to calculate the potentials inside and outside Σ so when $\kappa = 0$ we use only φ on Σ.

3. Numerical Solution of the Integral Equation

Boundary Element Method

The integral equations can be solved numerically by the boundary element method. The first step is to partition the surface into surface elements. These can be of arbitrary shape but are usually taken as simple polygons like triangles or rectangles. Later on we describe a triangulation procedure applicable to the surface of macromolecules. As a second step the unknown functions φ and h are approximated in some finite dimensional space by continuous trial functions $\hat{\varphi}$ and $\hat{h}$. Here we only consider the case that on each surface element the functions $\hat{\varphi}$ and $\hat{h}$ are polynomials uniquely determined by their values at a number of nodes. On a triangle we can take, for example, $a_1 + a_2 x + a_3 y$ as polynomial with the three vertices as nodes.

As basis function $S_k(\mathbf{r})$ we take the trial function which equals 1 at the kth node and zero at all other nodes. This is a kind of pyramid function only nonzero on the elements containing the kth node. The trial functions $\hat{\varphi}$ and $\hat{h}$ can both be expressed in one and only one way as linear combinations

$$\hat{\varphi}(\mathbf{r}) = \sum_{k=1}^{n} a_k S_k(\mathbf{r}) \tag{3.1}$$

and

$$\hat{h}(\mathbf{r}) = \sum_{k=1}^{n} b_k S_k(\mathbf{r}), \tag{3.2}$$

where n is the total number of nodes.

To determine the unknown coefficients a_k and b_k we use the so-called collocation method in which the trial functions $\hat{\varphi}$ and $\hat{h}$ satisfy the integral equations exactly in n points (the *collocation points*). The integrals in (2.17) and (2.18) are now written as sums of integrals over elements, which results in a set of linear equations for the coefficients a_k and b_k:

$$\begin{pmatrix} \mathbf{a} \\ \mathbf{b} \end{pmatrix} - \begin{pmatrix} \mathbf{A}_1 & \mathbf{A}_2 \\ \mathbf{A}_3 & \mathbf{A}_4 \end{pmatrix} \begin{pmatrix} \mathbf{a} \\ \mathbf{b} \end{pmatrix} = \begin{pmatrix} \mathbf{c} \\ \mathbf{d} \end{pmatrix}. \tag{3.3}$$

Here $\mathbf{a}$ and $\mathbf{b}$ are the unknown vectors a_k and b_k, $\mathbf{A}_1$ to $\mathbf{A}_4$ are matrices of local surface integrals involving the kernels L_1 to L_4, respectively, and $\mathbf{c}$ and $\mathbf{d}$ are the source terms on the r.h.s. of (2.17) and (2.18).

This set of equations can be written as a single matrix equation of dimension $2n$, where n is the number of collocation points,

$$(\mathbf{I} - \mathbf{A})\mathbf{x} = \mathbf{p}, \tag{3.4}$$

which can be solved by standard LU-decomposition methods. We note that $\mathbf{A}$ is determined by the surface only and not by the source term, so that for any surface geometry the decomposition of $\mathbf{I} - \mathbf{A}$ is required only once. The vector $\mathbf{x}$ represents the charge and dipole densities on the surface, which act as a source for the reaction field.

The internal potential $\varphi(\mathbf{r}_0^-)$ is given by Eq. (2.20),

$$\varphi(\mathbf{r}_0^-) = \sum_{j=1}^{2n} t_j x_j + \varphi^{\mathrm{C}}(\mathbf{r}_0^-), \tag{3.5}$$

where the t_j's are local surface integrals representing the potential of the surface charge and dipole densities, and φ^{C} is the direct Coulomb interaction. The external potential (2.23) can be expressed in a similar way.

Peak Separation for Charges near the Surface

As will become clear from the next section, numerical inaccuracy increases sharply when a source charge comes close to the surface. This is due to the strong variations in φ and especially in h. Zauhar and Morgan treat this difficulty by taking a local refinement of the elements near a charge. In realistic problems there are hundreds of charges and such local refinements will be needed frequently, increasing the number of unknowns. Moreover, the grid on Σ should be reconsidered when-

ever the positions of the charges change. Therefore, instead of using a local refinement for the approximation of h on Σ, we will split h into a smooth, or weakly varying, part $\tilde{h}$ and a non-smooth, or strongly varying, part $\bar{h}$. Hence $h = \tilde{h} + \bar{h}$. This splitting or "peak separation" can be done such that $\bar{h}$ is a known function and therefore its contribution only shows up in the right-hand side of the equations. Because the remaining $\tilde{h}$ is smooth, we can use a rather coarse grid on Σ, thereby reducing the number of unknowns.

A similar procedure can be followed for φ as well, although for small values of κ the function φ is smooth in comparison with h.

If we substitute $h = \tilde{h} + \bar{h}$ and $\varphi = \tilde{\varphi} + \bar{\varphi}$ in (2.17) and (2.18) we obtain

$$\frac{1}{2}(1+\varepsilon)\,\tilde{\varphi}(\mathbf{r}_0) - \iint_{\Sigma} [L_1(\mathbf{r};\mathbf{r}_0)\,\tilde{\varphi}(\mathbf{r}) + L_2(\mathbf{r};\mathbf{r}_0)\,\tilde{h}(\mathbf{r})]\,d\mathbf{r}$$

$$= \iint_{\Sigma} [L_1(\mathbf{r};\mathbf{r}_0)\,\bar{\varphi}(\mathbf{r}) + L_2(\mathbf{r};\mathbf{r}_0)\,\bar{h}(\mathbf{r})]\,d\mathbf{r} + \sum_i q_i \{F(\mathbf{r}_i;\mathbf{r}_0) - P(\mathbf{r}_i;\mathbf{r}_0)\} \tag{3.6}$$

and

$$\frac{1}{2}(1+1/\varepsilon)\,\tilde{h}(\mathbf{r}_0) - \iint_{\Sigma} [L_3(\mathbf{r};\mathbf{r}_0)\,\tilde{\varphi}(\mathbf{r}) + L_4(\mathbf{r};\mathbf{r}_0)\,\tilde{h}(\mathbf{r})]\,d\mathbf{r}$$

$$= \iint_{\Sigma} [L_3(\mathbf{r};\mathbf{r}_0)\,\bar{\varphi}(\mathbf{r}) + L_4(\mathbf{r};\mathbf{r}_0)\,\bar{h}(\mathbf{r})]\,d\mathbf{r}. \tag{3.7}$$

Appendix A motivates the following choice for $\bar{h}$ and $\bar{\varphi}$:

$$\bar{h}(\mathbf{r}) = \frac{2\varepsilon}{1+\varepsilon} \sum_i q_i \frac{\partial F}{\partial n_0}(\mathbf{r}_i;\mathbf{r}); \qquad h(\mathbf{r}) = \tilde{h}(\mathbf{r}) + \bar{h}(\mathbf{r}) \tag{3.8}$$

and

$$\bar{\varphi}(\mathbf{r}) = \frac{2}{1+\varepsilon} \sum_i q_i P(\mathbf{r}_i;\mathbf{r}); \qquad \varphi(\mathbf{r}) = \tilde{\varphi}(\mathbf{r}) + \bar{\varphi}(\mathbf{r}) \tag{3.9}$$

Once φ and h on Σ have been calculated we can obtain the potentials inside and outside Σ using (2.20) and (2.23), in which (3.8) and (3.9) are substituted.

A Triangulation Procedure

Unless simple parameterization is possible, the generation of a surface which forms the boundary between a discrete region and a continuum is a complicated matter. The most difficult part is to obtain a proper triangulation. The calculation of a dotted surface is standard; the Connolly program [24], for instance, calculates the solvent-accessible surface of a macromolecule and produces a set of dots and unit normal vectors. One could try to form triangles directly from the dots, as

Zauhar and Morgan have done, but success is not guaranteed, especially at low dot densities.

Since we are interested in a relatively small number of elements, we follow a different procedure. The triangulation is performed in three steps. The first step is the calculation of a high-density dot surface of the macromolecule, using the Connolly program or any other procedure. The second step is the definition of a triangulated grid on the surface of a sphere, e.g., from a regular polyhedron. Any spherical triangulation with the required density is acceptable. The vectors of the vertices and the dots are translated to a common origin, for instance, the center of mass of the macromolecule. The vectors of the vertices on the sphere are referred to as *spokes*. The third step is to assign the nearest surface point or dot to each spoke. This is done by testing the scalar product of the spoke and dot unit vectors, which should be positive and near to one, and then selecting the surface point with the shortest distance to the spoke. If required, triangles can be subdivided to refine the grid locally.

The position vector of the dot found in this way replaces the original position vector of the spoke and the accompanying normal vector is also assigned to the spoke. In this way all spokes are replaced by surface points of the macromolecule and a triangulated boundary is obtained. The method works for surfaces that are not too irregular in the sense that each spoke must intersect the surface only once.

Computation of the Matrix Elements

For the computation of matrix elements of **A** in Eq. (3.4) and the local surface integrals t_j in Eq. (3.5) three choices must be made. The first concerns the approximation of the surface based on the nodes or triangulation points and the normals in these points. The second choice concerns the positions of the collocation points, for which we simply take the grid points. The third choice is the form of the basis functions, which we take as piecewise linear functions in a triangular element and bilinear functions in a quadrilateral element, with the value 1 in one node and 0 in the others. The usual finite-element procedures [25] involve transformation of surface elements into a standard element on which the basis functions are defined.

4. Test for a Spherical Model

To understand what are really the important characteristics of the problem, we will consider some numerical results for the simple case in which Σ is the surface of a sphere. For this case an analytic solution is available and so we can in fact calculate the numerical errors.

With a sphere it is convenient to use spherical coordinates (r, β, θ). Without loss of generality, we can take the radius of the sphere equal to one unit (this implies a practical range of interest for κ of $0 \leqslant \kappa \leqslant 10$; the highest value would occur for a sphere of 3-nm radius in a medium with a Debye length of 0.3 nm). The elements

of the matrices $\mathbf{A}_1$ to $\mathbf{A}_4$ (Eq. (3.3)) contain integrals over Σ which can be obtained by a summation of integrals over single surface elements $\Sigma_{ij} = (\beta_i, \beta_{i+1}) \times (\theta_j, \theta_{j+1})$ of the form

$$\iint_{\Sigma_{ij}} L_s(\beta, \theta; \beta^0, \theta^0)\, S_{kl}(\beta, \theta) \sin(\beta)\, d\beta\, d\theta,$$

where (β^0, θ^0) denotes a collocation point and the basis functions S_{kl} are piecewise bilinear functions. In these integrals over Σ_{ij} we can restrict ourselves to $k = i, i+1$; $l = j, j+1$, since otherwise $S_{kl} \equiv 0$.

To calculate these integrals we used a Gauss product rule that works fine for smooth functions. However, as is apparent from the formulas in Section 2, some integrands are singular of order $1/|\mathbf{r} - \mathbf{r}_0|$ for $\mathbf{r} \to \mathbf{r}_0$. These singularities are integrable but difficult to handle numerically. We solved this problem by using some appropriate coordinate transformations [26], that make the integrands non-singular (these new coordinates are similar to polar coordinates). Consider as an illustration of this the surface $[0, 1] \times [0, 1]$ with coordinates β and θ and a collocation point $\mathbf{r}_0$ in (0, 0). We divide the surface in two parts:

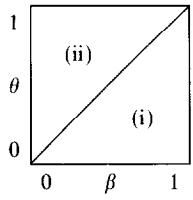

We can write the singularity $1/|\mathbf{r} - \mathbf{r}_0|$ for $\mathbf{r} \to \mathbf{r}_0$ in (i) as $1/\beta$ for $\beta \to 0$, and in (ii) as $1/\theta$ for $\theta \to 0$. In (i) we use the transformation $(\beta, \theta) \to (\beta, \eta)$ with $\eta = \arctan(\theta/\beta)$, so $d\beta\, d\theta$ becomes $\beta/\cos^2 \eta\, d\beta\, d\eta$ and the singularity is removed. In (ii) we use the transformation $(\beta, \theta) \to (\eta, \theta)$, with $\eta = \arctan(\beta/\theta)$, so $d\beta\, d\theta$ becomes $\theta/\cos^2 \eta\, d\eta\, d\theta$.

Now all the parameters in the set of equations can be calculated in a proper way and this leads to a very well-conditioned system of equations, which can be solved easily by Gaussian elimination.

We use the method without peak separation to solve the following problem. For Σ we take the surface of a sphere with a radius of 1 unit, and inside Σ there is one charge at distance r_c from the center of the sphere. The charge approaches Σ, so r_c tends to 1. By taking the expression for φ in (2.20) minus the last term, we get the reaction potential. We calculate this at the same point where the charge is located. This point is located below the center of one of the largest elements because we want to study the case which is numerically the most difficult one. The results are given in Table I. This table shows the exact solution as obtained from [8] together with the numerical results from the method mentioned above and the relative errors in these results.

TABLE I

Numerical Results for the Reaction Potential at the Site of a Single Charge inside Σ, Located at r_c from the Center of the Sphere of Radius 1

r_c	Num. method	Exact sol.	Rel. err (%)	$\|\varphi-\hat{\varphi}\|_{\text{rel}}$ (%)	$\|h-\hat{h}\|_{\text{rel}}$ (%)
0.00	−0.07858	−0.07858	−0.000	0.0	0.0
0.10	−0.07934	−0.07936	−0.017	0.3	0.1
0.20	−0.08172	−0.08178	−0.070	0.5	0.1
0.30	−0.08602	−0.08617	−0.165	0.8	0.2
0.40	−0.09287	−0.09317	−0.316	1.0	0.2
0.50	−0.10345	−0.10405	−0.574	1.3	0.3
0.60	−0.12010	−0.12142	−1.089	1.5	0.3
0.70	−0.14759	−0.15141	−2.520	2.5	0.6
0.75	−0.16799	−0.17573	−4.406	4.9	1.2
0.80	−0.19446	−0.21237	−8.430	12.1	2.8
0.85	−0.22740	−0.27347	−16.848	31.1	7.0
0.90	−0.26344	−0.39538	−33.372	74.2	16.2

Note. No splitting of φ and h applied; $\kappa = 3$, $\varepsilon = 20$, 200 elements.

The last two columns give the values of the relative one-norms of the errors

$$\|\varphi-\hat{\varphi}\|_{\text{rel}} = \iint_{\Sigma} |\varphi(\mathbf{r})-\hat{\varphi}(\mathbf{r})|\, d\mathbf{r} \Big/ \iint_{\Sigma} |\varphi(\mathbf{r})|\, d\mathbf{r}$$

and

$$\|h-\hat{h}\|_{\text{rel}} = \iint_{\Sigma} |h(\mathbf{r})-\hat{h}(\mathbf{r})|\, d\mathbf{r} \Big/ \iint_{\Sigma} |h(\mathbf{r})|\, d\mathbf{r}.$$

The surface Σ is divided into 200 elements (which implies an element side of 0.314 units) and we take $\kappa = 3$ and $\varepsilon = 20$. From the results we conclude that the method works very well as long as there are no charges close to Σ. When a charge approaches Σ, the approximation of the reaction potential appears to have a very large relative error.

To understand why the approximation of the functions φ and h on Σ becomes so difficult when a charge comes close to Σ, we study the situation in which one unit charge is located at the point $(r, \beta, \theta) = (0.9, 0, 0)$. Again we take $\kappa = 3$ and $\varepsilon = 20$. We have calculated $\varphi(\beta)$, $\bar{\varphi}(\beta)$, $\tilde{\varphi}(\beta)$, $h(\beta)$, $\bar{h}(\beta)$, and $\tilde{h}(\beta)$ on Σ in the points $(r, \beta, \theta) = (1, \beta, 0)$, using the exact solution given in [8]. The results are shown in Fig. 1. From this figure we conclude that $\bar{\varphi}$ and $\bar{h}$ are accurate approximations of φ and h, respectively. The peaks in $\tilde{\varphi}$ and $\tilde{h}$ are considerably smaller than the peaks in φ and h (Figs. 1C and F. Note the difference in the scale of the y-axis). By comparing Figs. 1A and D we see that the peak in h is stronger and more local than the peak in φ. As a result, h on Σ will be more difficult to approximate with bilinear basis functions than φ on Σ. However, by comparing the last two columns of

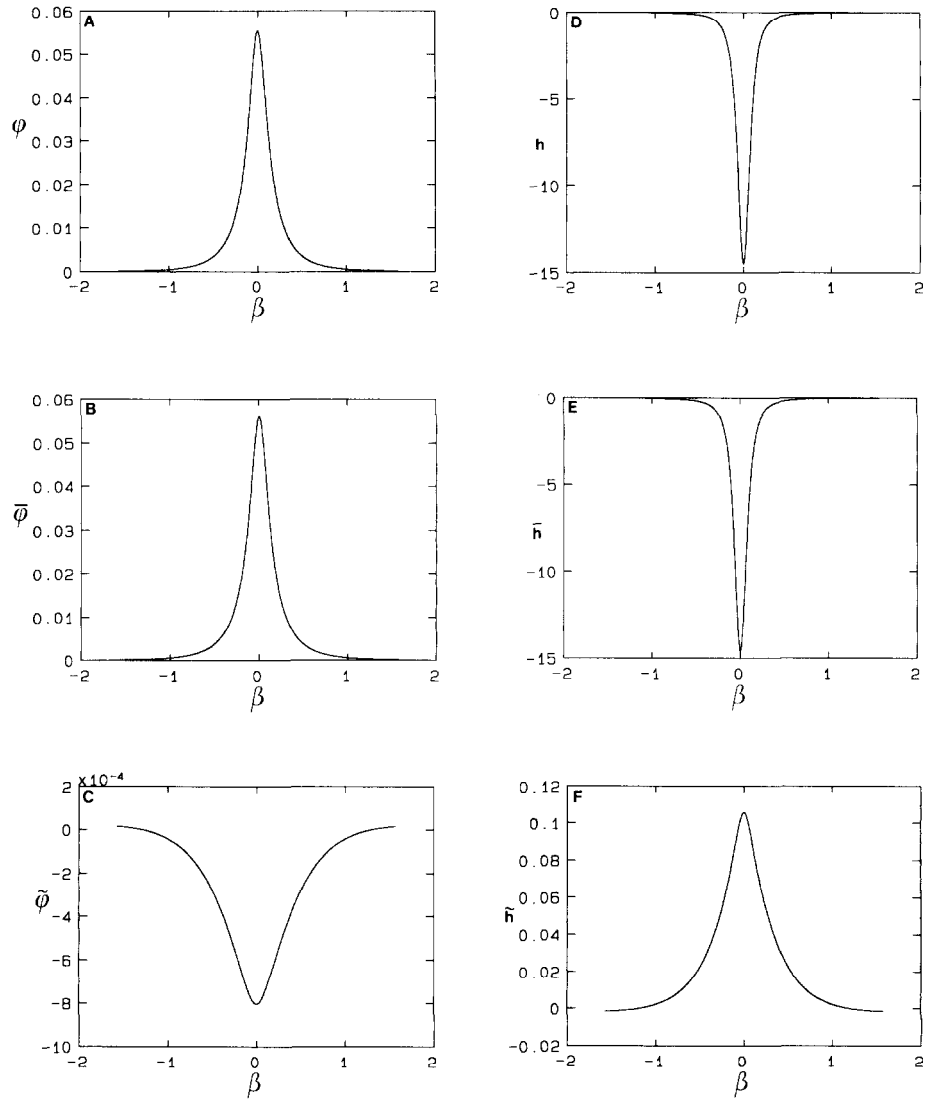

FIG. 1. The functions φ, $\bar{\varphi}$, $\tilde{\varphi}$ and h, $\bar{h}$, $\tilde{h}$ on Σ with a single charge inside Σ, against the polar coordinate β (see text).

TABLE II

Numerical Results as in Table I

r_c	Num. method	Exact sol.	Rel. err (%)	$\|\varphi-\hat{\varphi}\|_{\text{rel}}$ (%)	$\|h-\hat{h}\|_{\text{rel}}$ (%)
0.75	−0.17228	−0.16981	+1.451	0.5	0.9
0.80	−0.20992	−0.20568	+2.062	0.5	1.1
0.85	−0.27392	−0.26576	+3.071	0.5	1.4
0.90	−0.40502	−0.38620	+4.873	0.6	1.9

Note. Splitting of φ and h; $\kappa = 0$, $\varepsilon = 20$, 72 elements.

Table I we can see that the relative error in h is smaller than the relative error in φ. This is caused by the fact that h is much larger in absolute value than φ. The absolute error we make by approximating h with bilinear basis functions dominates the absolute error in φ because the integral equations to calculate φ and h on Σ are coupled. For $\kappa = 0$ the integral equations are decoupled and in that case the relative error in φ is smaller than the relative error in h. With $\kappa = 0$, for a single unit charge at a distance $r_c = 0.9$ from the origin and using again 200 elements we find $\|\varphi - \hat{\varphi}\|_{\text{rel}} = 1.1\,\%$ and $\|h - \hat{h}\|_{\text{rel}} = 14.9\,\%$.

Tables II and III show the results for the same problem mentioned earlier but using peak-separation and 72 elements, which implies a largest element side of 0.524 units. In Table II we take $\kappa = 0$ and in Table III, $\kappa = 3$. To show how the results improve by using more elements, Table IV shows the results when we divide Σ into 200 elements.

By comparing the results listed in Tables I and IV we conclude that splitting of φ and h makes the results considerably more accurate, although the calculation of the right-hand side of Eqs. (3.6) and (3.7) is more costly. Even with a smaller number of elements (Table III), the results are more accurate than the results obtained without peak-separation.

TABLE III

Numerical Results as in Table I

r_c	Num. method	Exact sol.	Rel. err (%)	$\|\varphi-\hat{\varphi}\|_{\text{rel}}$ (%)	$\|\varphi-\hat{\varphi}\|_{\text{rel}}$ (%)
0.75	−0.17556	−0.17573	−0.097	1.9	0.9
0.80	−0.21238	−0.21237	+0.005	2.9	1.1
0.85	−0.27448	−0.27347	+0.366	4.7	1.4
0.90	−0.40046	−0.39538	+1.284	7.3	2.0

Note. Splitting of φ and h; $\kappa = 3$, $\varepsilon = 20$, 72 elements.

TABLE IV

Numerical Results as in Table I

r_c	Num. method	Exact sol.	Rel. err (%)	$\|\varphi - \hat{\varphi}\|_{rel}$ (%)	$\|h - \hat{h}\|_{rel}$ (%)
0.75	−0.17561	−0.17573	−0.065	0.5	0.2
0.80	−0.21224	−0.21237	−0.057	0.6	0.2
0.85	−0.27360	−0.27347	+0.045	1.1	0.3
0.90	−0.39716	−0.39538	+.448	2.4	0.7

Note. Splitting of φ and h; $\kappa = 3$, $\varepsilon = 20$, 200 elements.

5. Application to a Protein

To test the applicability of the method to a realistic problem, we computed the electric potential at specific sites within the protein azurine, which is a copper-containing protein involved in electron transfer reactions. Two histidine residues in the protein are titratable; i.e., their acid strength or pK-values can be experimentally determined. This has been done by Groeneveld *et al.* [27] for both oxidation states of the copper (Cu^+ and Cu^{++}) in a solution with ionic strength between 0.02 and 0.04 molar. The pK-value, being a measure for the free energy of binding of a positively charged proton, will shift when the copper is oxidized because the energy of the bound proton in the potential of the copper ion will change. A proper calculation of this potential will predict the shift. A reason to choose azurin is that this pK-shift has been calculated by Bashford *et al.* ([28], henceforth referred to as BKC) using the finite-difference method, which enables a comparison with our method.

Structure, Surface Definition, and Integration

The coordinates at 0.18 nm resolution [29] of azurin from *Alcaligenes denitrificans* (129 amino acids) were taken from the Brookhaven Databank. Water molecules were not included. Polar hydrogens were generated by a program of the GROMOS package [30]. The Connolly program [24] was used to calculate the dot surface of the protein using a very high dot density of 400 to 600 nm^{-2} and a probe radius of 0.14 nm. On the average this resulted in 25,000 surface dots. Triangulation was carried out as described in Section 3, for 310 and 736 elements (157 and 370 nodes, respectively). The average boundary element size was about 0.5 nm for 310 elements and 0.3 nm for 736 elements. The method of "peak separation" (Section 3) was used throughout.

Since the reaction field is quite sensitive to the atomic radii used to construct the surface, we compared two sets of atomic radii, indicated by GR for values from the GROMOS force field and by CH for values from the CHARMm force field [31]. The latter values, which are smaller than the former, should be relevant for comparison with the calculations of BKC. The values of the radii of the relevant

atoms and their distances to the triangulated surface are given in Tables V and VI, respectively.

The procedure described by Zauhar and Morgan [18] was followed to describe the surface within each element by interpolation with a third-degree polynomial that preserves continuity of the normal to the surface. Integrals were evaluated by a Gaussian quadrature. In the case of the evaluation of L_1 and L_4 (Eqs. (2.17) and (2.18)) the singularity at the node was treated in a way similar to that described in Section 4.

Computation of pK-shift

The electrostatic calculations were carried out using relative dielectric constants of 4 for the molecular region and 80 for the electrolyte region, with ionic strengths ranging from 0 to 0.04 molar. The same values were used by BKC. The electric potential due to a charge on the copper was calculated on the atoms of three histidine rings (His 32, 35, and 83). In order to compare with BKC, we computed the pK-shift resulting from the potential on the Nδ and Nε nitrogen atoms. In addition we computed the pK-shifts resulting from a more realistic charge distribution over the histidine atoms for the protonated and unprotonated form of histidine, using GROMOS partial atomic charges (Table V). Although the charge on the copper site is also distributed over nearby atoms, we considered the copper as a point charge. The pK-shift of a histidine on oxidation of copper is given by

$$\Delta pK = pK(Cu^{2+}) - pK(Cu^{+}) = -\frac{F}{RT \ln 10} \sum_k \Delta z_k \varphi_k,$$

TABLE V

Charges and Radii of Relevant Atoms

	Charges[a]			Radii[b]	
Atom	HISδ	HISε	HIS[c]	GR[d]	CH[e]
Cγ	+0.13	+0	−0.05	0.19	0.18
Nδ_1	−0.58	+0	+0.30	0.23	0.16
Hδ_1	+0	+0.19	+0.30	0	0.08
Cε_1	+0.26	+0.26	−0.24	0.21	0.18
Nε_2	+0	−0.58	+0.31	0.23	0.16
Hε_2	+0.19	+0	+0.30	0	0.08
Cδ_2	+0	+0.13	+0	0.21	0.18
Cu		2		0.20	

[a] GROMOS partial charges.
[b] Atomic radii in nanometers.
[c] Histidine after addition of hydrogen at N_δ or N_ε.
[d] Atomic radii from the GROMOS program package [30].
[e] Atomic radii from the CHARMm program package [31].

TABLE VI

Shortest Distance of the Relevant Atoms to the Triangulated Surface[a]

Residue Atom	His 32		His 35		His 83	
	GR[b]	CH[c]	GR[b]	CH[c]	GR[b]	CH[c]
Cγ	0.18	0.15	0.51	0.47	0.26	0.22
	0.18	0.16	0.56	0.50	0.27	0.23
$N\delta_1$	0.17	0.12	0.50	0.45	0.24	0.21
	0.18	0.16	0.49	0.41	0.25	0.23
$H\delta_1$	0.12	0.07	0.43	0.40	0.27	0.21
	0.16	0.14	0.41	0.32	0.25	0.22
$C\varepsilon_1$	0.19	0.16	0.52	0.45	0.14	0.14
	0.18	0.16	0.50	0.43	0.20	0.18
$N\varepsilon_2$	0.21	0.20	0.60	0.50	0.16	0.14
	0.22	0.17	0.57	0.50	0.22	0.15
$H\varepsilon_2$	0.18	0.19	0.60	0.51	0.14	0.12
	0.21	0.15	0.57	0.50	0.18	0.12
$C\delta_2$	0.19	0.19	0.60	0.53	0.18	0.14
	0.19	0.18	0.59	0.48	0.20	0.18
Cu	(310 elements) CH 0.53 GR 0.61		(736 elements) CH 0.52 GR 0.59			

[a] The first row of each atom gives the distance in nanometers for a triangulation with 310 elements; the second row for 736 elements.

[b] Atomic radii from the GROMOS program package [30].

[c] Atomic radii from the CHARMm program package [31].

where φ_k is the potential on the kth atom of the histidine due to a positive charge of 1 elementary unit at the copper site, and Δz_k is the change in partial charge (in units of the elementary charge e) on the kth atom of histidine on going from the neutral to the protonated form. It is not known experimentally which of the two possible sites (the Nδ or the Nε ring nitrogen) is actually protonated. We considered the following cases:

Nδ: only Nδ-position, with $\Delta z = +1$;

Nε: only Nε-position, with $\Delta z = +1$;

Hisδ: all charge modifications for His atoms, for protonation on Nδ;

Hisε: all charge modifications for His atoms, for protonation on Nε.

Results

Table VII gives the resulting pK-shifts, using 736 boundary elements, and for three values of the ionic strength, corresponding to κ values of 0, 0.46, and 0.65 nm^{-1}, respectively. Comparison with our results with BKC show reasonable agreement for His 32 and moderate agreement for His 83; comparison with experi-

ment indicates that in both cases the ε-nitrogen is protonated. For His 83 the latter is in agreement with the fact that the Nε points towards the solution while the Nδ points inward; for His 32 this is not clear from the X-ray structure. The differences using the two sets of atomic radii, and using the two different surface constructions, give an indication of the sensitivity to the exact location of the surface. These differences are not very significant.

The values for His 35 differ considerably from BKC. This histidine is located more internally in the protein and at a shorter distance from the copper; experimentally no protonation is found. It is likely that the 0.1 nm grid used by BKC treats certain parts of space as external that in our procedure would be considered internal, e.g., at sites where water molecules have been observed. This would decrease the potential more strongly at internal sites.

Results for 310 elements (not shown) agree within 10 to 20% with the ones in Table VII, except for Nε of His 83 using CHARMm radii, for which a shift of 0.19 was found for 310 elements compared to 0.38 for 736 elements. Using the larger GROMOS radii no difference was found (0.38). Apparently the potential at this site is quite sensitive to the exact location of the surface. Although for Nε of His 83 our

TABLE VII

Absolute Values of pK-shifts of Histidines in Azurin on Oxidation of Copper[a]

		$I = 0.00$ M[b]			$I = 0.02$ M[b]			$I = 0.04$ M[b]			
Res.	Atom[c]	GR[d]	CH[e]	BKC[f]	GR	CH	BKC	GR	CH	BKC	Exp[g]
His 32	Nδ	0.27	0.19	0.18	0.19	0.14	0.099	0.17	0.13	0.086	
	Hisδ	0.27	0.19		0.19	0.14		0.17	0.13		0.07
	Nε	0.18	0.15	0.16	0.12	0.097	0.080	0.10	0.088	0.068	
	Hisε	0.19	0.16		0.13	0.10		0.11	0.093		
His 35	Nδ	2.68	2.28	1.28	2.58	2.24	1.19	2.54	2.24	1.17	
	Hisδ	2.80	2.41		2.71	2.37		2.67	2.37		
	Nε	3.91	3.51	1.78	3.81	3.47	1.69	3.77	3.46	1.67	
	Hisε	3.83	3.43		3.73	3.38		3.69	3.38		
His 83	Nδ	0.95	0.89	0.54	0.87	0.82	0.46	0.85	0.81	0.44	
	Hisδ	0.96	0.90		0.89	0.84		0.87	0.83		0.25
	Nε	0.41	0.45	0.28	0.38	0.39	0.20	0.37	0.38	0.18	
	Hisε	0.50	0.53		0.47	0.47		0.46	0.47		

[a] 736 boundary elements.

[b] Ionic strength in molar.

[c] N_δ and N_ε. Positive charge on N_δ and N_ε of histidine only His_δ and His_ε; distributed charge on histidine atoms, $_\delta$ or $_\varepsilon$ protonated.

[d] GROMOS atomic radii.

[e] CHARMm atomic radii.

[f] Finite difference method from Ref. [28].

[g] Experimental values from Ref. [27] (ionic strength between 0.02 and 0.04).

result for 310 elements happens to agree well with BKC, we note that in such cases a continuum treatment cannot be trusted anymore and a refinement of the solvent interaction is necessary.

6. Discussion

In the computation of the electric potential for a macromolecule in a solvent with given ionic strength the number of unknowns can be reduced by an order of magnitude, compared to finite-difference methods, by formulating the problem as two coupled integral equations on the surface Σ. These equations can be solved by straightforward application of boundary element techniques, yielding quite accurate results as long as the charges do not approach the surface much closer than the element size.

Finite-difference methods as used in [11–13 and 28] distribute charges over grid points. This inevitably results in large errors in the total potential at points close to any charge [13]. In addition, self-energy terms cannot be computed in an unambiguous way. With boundary element methods these problems do not occur since a direct Coulomb term is included. Remaining errors arise exclusively from errors in the reaction field.

When a charge gets close to the surface, strong local variation of the exact solution will occur and any numerical method will require special considerations to preserve accuracy in that case. In our method we treat this problem by splitting the unknown functions φ and h in a smooth and a non-smooth part. By doing this the surface grid can be taken quite coarse, thus reducing the numerical effort required to solve the integral equations, but the computation of the right-hand side of (3.6) and (3.7) becomes more complex and time consuming. In practical cases there is an optimum if refining of the grid is compared to this method of "peak separation." This optimum depends on the required accuracy and on the way the local surface integrals are evaluated.

The results can depend quite critically on the exact location and description of the surface if charges are very close to the interface. It is clear that in such cases the physical validity of the continuum approximation is also questionable. For physical applications it makes no sense to refine the numerical accuracy of a mathematical model beyond the physical validity of the model itself. Therefore we will consider the limits of the model itself.

The correct computation of the electric potential of a macromolecule is necessary to describe the total hamiltonian of the system needed for simulations and for estimation of thermodynamic quantities. In this respect the electric potential represents the long-range part of the *potential of mean force*, which describes the interaction free energy of the particles with the solvent. But such a potential of mean force also has a short-range part that should make up the difference between the total free energy of interaction with the solvent and the long-range part. Thus there is a certain freedom of choice in dividing the total interaction potential

between these two parts. The choice was made here to treat the solvent as a continuum with linear dielectric and Poisson–Boltmann response. This implies that solvent molecules with deviating behaviour should not be considered part of the continuum, but should be incorporated into the "macromolecule" itself.

The boundary with the continuum should not be chosen so close to the actual charges that the reaction field shows very strong peaks, which are physically unrealistic and need compensation in the short-range terms. Thus, in realistic applications, it is advantageous to define a boundary layer between the real atoms and the continuum, which prevents unphysical behaviour of the continuum and forms the site of the short-range part of the potential of mean force.

We note that the continuum equations describe the low-frequency behaviour of the electric potential. Both the induced dipole density and the induced charge density in the solvent are the result of dynamic processes, leading to a frequency-dependent response. The incorporation of the electric potential based on the equations given here will correctly describe thermodynamic equilibrium properties. For correct dynamic responses further refinements are necessary.

7. Conclusion

A boundary element method is presented to compute the potential φ at any position for a set of charges q_i located at positions $\mathbf{r}_i$ in a homogeneous dielectricum (with dielectric constant ε_1) which is separated by an arbitrarily shaped boundary Σ from an environment with different dielectric constant ε_2 and with linearized Poisson–Boltzmann behaviour corresponding to a given ionic strength characterized by an inverse Debye length κ. The resulting equations on Σ can be summarized as

$$\frac{1}{2}(1+\varepsilon_2/\varepsilon_1)\,\varphi(\mathbf{r}_0) = \iint_\Sigma \{F(\mathbf{r};\mathbf{r}_0) - P(\mathbf{r};\mathbf{r}_0)\}\,\frac{\partial\varphi}{\partial n}(\mathbf{r})\,d\mathbf{r} + \iint_\Sigma \left\{\frac{\partial P}{\partial n}(\mathbf{r};\mathbf{r}_0)\,\varepsilon_2/\varepsilon_1 - \frac{\partial F}{\partial n}(\mathbf{r};\mathbf{r}_0)\right\}\varphi(\mathbf{r})\,d\mathbf{r} + \sum_i q_i F(\mathbf{r}_i;\mathbf{r}_0)/\varepsilon_1$$

and

$$\frac{1}{2}(1+\varepsilon_1/\varepsilon_2)\,\frac{\partial\varphi}{\partial n}(\mathbf{r}_0) = \iint_\Sigma \left\{\frac{\partial F}{\partial n_0}(\mathbf{r};\mathbf{r}_0) - \frac{\partial P}{\partial n_0}(\mathbf{r};\mathbf{r}_0)\,\varepsilon_1/\varepsilon_2\right\}\frac{\partial\varphi}{\partial n}(\mathbf{r})\,d\mathbf{r} + \iint_\Sigma \left\{\frac{\partial^2 P}{\partial n_0\,\partial n}(\mathbf{r};\mathbf{r}_0) - \frac{\partial^2 F}{\partial n_0\,\partial n}(\mathbf{r};\mathbf{r}_0)\right\}\varphi(\mathbf{r})\,d\mathbf{r} + \sum_{i=1}^{N} q_i \frac{\partial F}{\partial n_0}(\mathbf{r}_i;\mathbf{r}_0)/\varepsilon_1$$

with

$$F(\mathbf{r};\mathbf{s}) = 1/(4\pi\,|\mathbf{r}-\mathbf{s}|) \qquad \text{and} \qquad P(\mathbf{r};\mathbf{s}) = e^{-\kappa|\mathbf{r}-\mathbf{s}|}F(\mathbf{r};\mathbf{s}).$$

Once $\varphi(\mathbf{r}_0)$ and $(\partial\varphi/\partial n)(\mathbf{r}_0)$ on Σ have been calculated we can calculate the potential in an interior point $\mathbf{r}_0^-$, using

$$\varphi(\mathbf{r}_0^-) = \iint_\Sigma \{F(\mathbf{r};\mathbf{r}_0^-) - P(\mathbf{r};\mathbf{r}_0^-)\}\frac{\partial\varphi}{\partial n}(\mathbf{r})\,d\mathbf{r} + \iint_\Sigma \left\{\frac{\partial P}{\partial n}(\mathbf{r};\mathbf{r}_0^-)\,\varepsilon_2/\varepsilon_1 - \frac{\partial F}{\partial n}(\mathbf{r};\mathbf{r}_0^-)\right\}\varphi(\mathbf{r})\,d\mathbf{r} + \sum_i q_i F(\mathbf{r}_i;\mathbf{r}_0^-)/\varepsilon_1,$$

and in an exterior point $\mathbf{r}_0^+$, using

$$\varphi(\mathbf{r}_0^+)\,\varepsilon_2\varepsilon_1 = \iint_\Sigma \{F(\mathbf{r};\mathbf{r}_0^+) - P(\mathbf{r};\mathbf{r}_0^+)\}\frac{\partial\varphi}{\partial n}(\mathbf{r})\,d\mathbf{r} + \iint_\Sigma \left\{\frac{\partial P}{\partial n}(\mathbf{r};\mathbf{r}_0^+)\,\varepsilon_2/\varepsilon_1 - \frac{\partial F}{\partial n}(\mathbf{r};\mathbf{r}_0^+)\right\}\varphi(\mathbf{r})\,d\mathbf{r} + \sum_i q_i F(\mathbf{r}_i;\mathbf{r}_0^+)/\varepsilon_1.$$

We conclude that the method presented here provides an accurate and efficient means to calculate the electric potential for charged macromolecules in solution and can be applied in potentials of mean force used for simulations.

Appendix A

In this section we want to derive expressions $\bar{h}$ and $\bar{\varphi}$ which yield accurate approximations for the local behaviour of φ and h, respectively, when a charge approaches Σ. First we derive a function $\bar{h}$. We therefore consider the second integral equation (2.18). Since we are only interested in the local behaviour of h, we neglect the influence of the curvature. In the integral equation the term with L_4 vanishes, because

$$L_4(\mathbf{r};\mathbf{r}_0) = \frac{\cos\theta_0}{4\pi\,|\mathbf{r}-\mathbf{r}_0|^2}(1 - e^{-\kappa|\mathbf{r}-\mathbf{r}_0|}(1+\kappa\,|\mathbf{r}-\mathbf{r}_0|)/\varepsilon)$$

and $\cos\theta_0 = 0$ in case Σ is a flat surface. Due to $\varphi \ll h$ the term with φ is small compared with the other terms in (2.18) so

$$h(\mathbf{r}_0) \approx \frac{2\varepsilon}{1+\varepsilon}\sum_i q_i \frac{\partial F}{\partial n_0}(\mathbf{r}_i;\mathbf{r}_0).$$

We now choose $\bar{h}(\mathbf{r})$ to be

$$\frac{2\varepsilon}{1+\varepsilon}\sum_i q_i \frac{\partial F}{\partial n_0}(\mathbf{r}_i;\mathbf{r}).$$

If we substitute the splitting of h in (2.17) and (2.18) we find

$$\frac{1}{2}(1+\varepsilon)\,\varphi(\mathbf{r}_0) - \iint_{\Sigma} [L_1(\mathbf{r};\mathbf{r}_0)\,\varphi(\mathbf{r}) + L_2(\mathbf{r};\mathbf{r}_0)\,\tilde{h}(\mathbf{r})]\,d\mathbf{r}$$

$$= \iint_{\Sigma} L_2(\mathbf{r};\mathbf{r}_0)\,\bar{h}(\mathbf{r})\,d\mathbf{r} + \sum_i q_i F(\mathbf{r}_i;\mathbf{r}_0) \tag{A.1}$$

and

$$\frac{1}{2}(1+1/\varepsilon)\,\tilde{h}(\mathbf{r}_0) - \iint_{\Sigma} [L_3(\mathbf{r};\mathbf{r}_0)\,\varphi(\mathbf{r}) + L_4(\mathbf{r};\mathbf{r}_0)\,\tilde{h}(\mathbf{r})]\,d\mathbf{r} = \iint_{\Sigma} L_4(\mathbf{r};\mathbf{r}_0)\,\bar{h}(\mathbf{r})\,d\mathbf{r}. \tag{A.2}$$

The known function $\bar{h}$ has been brought to the right-hand side of the equation. Unknown functions are now φ and $\tilde{h}$, which we approximate again with bilinear basis functions. The advantage of this method is that the variation in $\tilde{h}$ is much less than the variation in h, so the number of elements can be taken much smaller when approximating $\tilde{h}$ instead of h. As a result from this splitting of h the final system of linear equations becomes much smaller. Although for small values of κ the function φ is smooth in comparison with h, a similar approach can be followed. First we need an expression which yields an accurate approximation for the local behaviour of φ when a charge approaches Σ. Therefore we derive the integral equation

$$\varphi(\mathbf{r}_0^-) = \iint_{\Sigma} \left[P(\mathbf{r};\mathbf{r}_0^-)\,h(\mathbf{r}) - \frac{\partial P}{\partial n}(\mathbf{r};\mathbf{r}_0^-)\,\varphi(\mathbf{r}) \right] d\mathbf{r}$$

$$+ \sum_i q_i P(\mathbf{r}_i;\mathbf{r}_0^-) + \kappa^2 \iiint_V P(\mathbf{r};\mathbf{r}_0^-)\,\varphi(\mathbf{r})\,d\mathbf{r} \tag{A.3}$$

(V is the area surrounded by Σ).

This equation can be obtained by taking a linear combination of (2.2) and (2.5) and applying Green's second theorem on the colume inside Σ. Subtracting ε times (2.19) from this equation and taking the limit $\mathbf{r}_0^- \uparrow \Sigma$ yields

$$\frac{1}{2}(1+\varepsilon)\,\varphi(\mathbf{r}_0) = (\varepsilon-1) \iint_{\Sigma} \frac{\partial P}{\partial n}(\mathbf{r};\mathbf{r}_0)\,\varphi(\mathbf{r})\,d\mathbf{r}$$

$$+ \kappa^2 \iiint_V P(\mathbf{r};\mathbf{r}_0)\,\varphi(\mathbf{r})\,d\mathbf{r} + \sum_i q_i P(\mathbf{r}_i;\mathbf{r}_0).$$

Because both $(\partial P/\partial n)(\mathbf{r};\mathbf{r}_0)$ and $P(\mathbf{r};\mathbf{r}_0)$ are $O(1/|\mathbf{r}-\mathbf{r}_0|)$ the first integral in the equation is $O(|\mathbf{r}-\mathbf{r}_0|)$ and the integral over V is $O(|\mathbf{r}-\mathbf{r}_0|^2)$. This implies that the last term in the above equation is the most important one in the right-hand side.

This leads to a function which approximates the local behaviour of φ when a charge comes near Σ and κ is small,

$$\bar{\varphi}(\mathbf{r}_0) = \frac{2}{1+\varepsilon} \sum_i q_i P(\mathbf{r}_i; \mathbf{r}_0).$$

We now write φ as $\tilde{\varphi}(\mathbf{r}) + \bar{\varphi}(\mathbf{r})$, and substitute this expression in (A.1) and (A.2), which leads to the desired equation.

ACKNOWLEDGMENTS

This work was supported in part by the Netherlands Foundation for Chemical Research (SON) with financial aid from the Netherlands Organization for Scientific Research (NWO). We are also grateful to S. J. H. Beukers and J. H. Hartmann from the department of mathematics and to J. P. Dijkman and P. Th. van Duijnen from the department of chemistry.

REFERENCES

1. W. G. J. HOL, P. TH. VAN DUIJNEN, AND H. J. C. BERENDSEN, *Nature (London)* **273,** 443 (1978).
2. W. G. J. HOL, *Prog. Biophys. Mol. Biol.* **45**, 149 (1985).
3. H. J. C. BERENDSEN, *Europhys. News* **17**, 8 (1986).
4. M. BORN, *Z. Phys.* **1**, 45 (1920).
5. J. G. KIRKWOOD AND F. H. WESTHEIMER, *J. Chem. Phys.* **6**, 506 (1938); F. H. WESTHEIMER AND J. G. KIRKWOOD, *J. Chem. Phys.* **6**, 513 (1938).
6. C. TANFORD AND J. G. KIRKWOOD, *J. Amer. Chem. Soc.* **79**, 5333 (1957); C. TANFORD, *J. Amer. Chem. Soc.* **79**, 5340, 5348 (1957).
7. A. WARSHEL AND S. T. RUSSEL, *Q. Rev. Biophys.* **17**, 283 (1984).
8. M. K. GILSON, A. RASHIN, R. FINE, AND B. HONIG, *J. Mol. Biol.* **183**, 503 (1985).
9. P. B. SHAW, *Phys. Rev. A* **32**, 2476 (1985).
10. K. SHARP AND B. HONIG, *Ann. Rev. Biophys. Chem.* **19**, 301 (1990).
11. J. WARWICKER AND H. C. WATSON, *J. Mol. Biol.* **157**, 671 (1982).
12. I. KLAPPER, R. HAGSTROM, R. FINE, K. SHARP, AND B. HONIG, *Proteins: Struct. Funct. Genet.* **1**, 47 (1986).
13. M. K. GILSON, K. A. SHARP, AND B. H. HONIG, *J. Comput. Chem.* **9**, 329 (1987).
14. H. NAKAMURA, *J. Phys. Soc. Japan* **57**, 3702 (1988).
15. C. A. BREBBIA AND S. WALKER, *Boundary Element Techniques in Engineering* (Newnes–Butterworths, London, 1980).
16. P. K. BANERJEE AND R. BUTTERFIELD, *Boundary Element Methods in Engineering Science* (McGraw–Hill, New York, 1981).
17. R. J. ZAUHAR AND R. S. MORGAN, *J. Mol. Biol.* **186**, 815 (1985).
18. R. J. ZAUHAR AND R. S. MORGAN, *J. Comput. Chem.* **9**, 171 (1988).
19. J. P. DIJKMAN, Ph. D. thesis, Chap. 5, University of Groningen, The Netherlands, 1989 (unpublished).
20. R. J. ZAUHAR, in *Electrostatics in Recognition Processes between Biological Macromolecules*, edited by E. Westhof, Centre Européen de Calcul. Atomique et Moléculaire, 68 (CECAM, Bât. 506, Université Paris-Sud, Orsay, France, 1987).
21. A. A. RASHIN, *J. Phys. Chem.* **94**, 1725 (1990).

22. J. P. VAN DER EERDEN, in *Nuclei Acid Conformation and Dynamics*, edited by W. Olson (CECAM, Orsay, France, 1983), p. 61 (see Ref. [19]).
23. I. STACKGOLD, *Boundary Value Problems of Mathematical Physics*, Vol. 2, MacMillan Series in Advanced Mathematics and Theoretical Phyics (MacMillan Co., New York, 1968).
24. M. L. CONNOLLY, *J. Appl. Cryst.* **18**, 499 (1985).
25. O. C. ZIENKIEWICZ, *The Finite Element Method* (McGraw–Hill, London, 1977).
26. E. F. F. BOTTA, *Calculation of Potential Flow around Bodies*, Ph.D. thesis, University of Groningen, The Netherlands, 1978 (unpublished).
27. C. M. GROENEVELD, M. C. OUWERLING, C. ERKELENS, AND G. W. CANTERS, *J. Mol. Biol.* **200**, 189 (1988).
28. D. BASHFORD, M. KARPLUS, AND G. W. CANTERS, *J. Mol. Biol.* **203**, 507 (1988).
29. G. E. NORRIS, B. F. ANDERSON, AND E. M. BAKER, *J. Am. Chem. Soc.* **108**, 2784 (1986).
30. W. F. V. GUNSTEREN AND H. J. C. BERENDSEN, *Groningen Molecular Simulation (GROMOS)*, available from BIOMOS, Nijenborgh 16, 9747 AG Groningen, The Netherlands, 1987 (GROMOS is a trademark of BIOMOS b.v.).
31. B. R. BROOKS, R. E. BRUCCOLERI, B. D. OLAFSON, D. J. STATES, S. SWAMINATHAN, AND M. KARPLUS, *J. Comput. Chem.* **4**, 187 (1983) (CHARMm is a trademark of Polygen Corporation).

581/97/1-12